Progress In Electromagnetics Research, Vol. 121, 433–452, 2011

OPTICAL RESPONSE OF A PERFECT CONDUCTOR WAVEGUIDE THAT BEHAVES AS A PHOTONIC CRYSTAL

A. Mendoza-Suárez[1], H. Pérez-Aguilar[1], and F. Villa-Villa[2, *]

[1]Facultad de Ciencias Físico-Matemáticas, Universidad Michoacana de San Nicolás de Hidalgo, Edificio B, Ciudad Universitaria, Morelia, Mich. 58060, México

[2]Centro de Investigaciones en Óptica, Loma del Bosque 115, León, Gto. 37150, México

Abstract—In this work, we consider a waveguide composed of two periodic, perfectly conducting, one-dimensional rough surfaces. This periodic system has a band structure similar in some aspects to a one-dimensional photonic crystal. However, our system has some additional interesting features. We calculate the band structure and the reflectivity of a corresponding finite waveguide. We found that the variation of the roughness amplitude and the relative phases allow to control at a certain degree the band structure of the system. Particularly, wide gaps can be obtained. It is even possible to obtain discrete modes for some frequency range and then the periodic waveguide acts as an unimodal filter. The system considered constitutes itself a photonic crystal whose band structure corresponds in many ways to a conventional photonic crystal but using just a single material. The key properties of this system are that it really constitutes a waveguide whose optical response is similar to that of a one-dimensional photonic crystal.

1. INTRODUCTION

The study of the interaction of electromagnetic waves with corrugated surfaces and resonators with corrugated walls of metals and perfect electric conductors (PEC) has been the subject of some studies during the past years [1–5], given their importance in the design of antennas and rectangular waveguides for macroscopic systems [6–8].

Received 24 August 2011, Accepted 17 October 2011, Scheduled 3 November 2011

* Corresponding author: Francisco Villa-Villa (fvilla@cio.mx).

During the last years, the study of nanostructured metals has given place to new research fields such as that of left handed materials [9]. It has also been shown theoretically and experimentally that nanostructured metals consisting on PEC with periodic two-dimensional arrays of holes, can support surface modes that are exclusively associated to the structure of the system [10–14].

Another field of structured materials that has recently arisen is related to photonic crystals. These systems that constitute periodic arrays of different materials with a unit cell of dimension on the order of the wavelength, have the potential to develop a new technology of integrated optical circuits [15]. A particular system that is closely related to the system proposed in this work was considered by Maradudin and McGurn [16]. They studied a truncated two-dimensional photonic crystal between two PEC surfaces of infinite extent separated by a given distance, and determined the band structure of this system by using a plane wave expansion. They found that the curves representing the characteristic modes get flatter when such distance is small, and in a similar way as happens with the system we are proposing, it is possible to get discrete modes at low frequencies, that is, when the cavity becomes narrow.

The geometry of the system proposed in this work, has been considered to constitute some billiard systems to study their quantum and classical transport properties [17, 18]. It is worth to mention that under certain conditions such systems can become chaotic.

In present work, we propose a nanostructured periodic waveguide with PEC corrugated walls. In the theory section we introduce an integral method to calculate the band structure of our system based on the ideas outlined elsewhere [19]. The integral method is also used to calculate the propagation of the electromagnetic field across a finite length waveguide [20]. In Section 3, we obtain numerical results by varying the geometric parameters of the walls of the corrugated waveguide to determine the optical response of the system. In Section 4, we present our conclusions.

2. THEORY

We consider a waveguide composed of two periodic, perfectly conducting, rough surfaces. The medium between the corrugated surfaces is vacuum (or any dielectric material). The system is sketched in Fig. 1.

We consider that the periodic profiles have a period P, the average width of the waveguide is given by b, and the surface profiles can be represented by the harmonic functions $b/2 + A_1 \cos(2\pi x/P)$ (upper

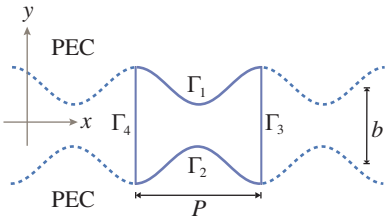

Figure 1. Graphic description of the waveguide between corrugated perfect conductor walls. The Γ contours define the unit cell of the system with periodicity in the x-direction.

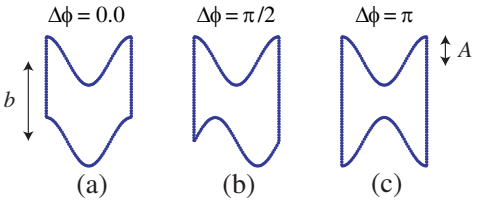

Figure 2. Unit cell profiles for different phase differences that will be considered in the examples.

profile) and $-b/2 + A_2 \cos(2\pi x/P - \Delta\phi)$ (lower profile), where A_1 and A_2 represent the amplitudes and $\Delta\phi$ stands for a phase difference between both profiles. The phase difference plays an important role in the optical response of our system. In Fig. 2, we show the unit cells for the phase differences $\Delta\phi = 0$ (Fig. 2(a)), $\Delta\phi = \pi/2$ (Fig. 2(b)), and $\Delta\phi = \pi$ (Fig. 2(c)) respectively.

Let us consider the problem of finding the band structure of the system. We use an integral method that can be formulated by following the same ideas developed elsewhere [19, 21, 22]. This problem can be studied using the scalar theory by considering two complementary polarization states given the symmetry of our physical system along the z-direction. We are interested in the response of the system when the only component of the electric field, E, is parallel to the direction of symmetry, that is in the case of TE polarization.

We assumed that the electric field E is time harmonic $E(\mathbf{r}, t) = \Psi(\mathbf{r}) e^{-i\omega t}$. Under this consideration it is well-known that the function $\Psi(\mathbf{r})$ satisfies the Helmholtz equation

$$\nabla^2 \Psi(\mathbf{r}) + \left(\frac{\omega}{c}\right)^2 \Psi(\mathbf{r}) = 0, \tag{1}$$

where ω is the frequency of the electromagnetic wave, c is the speed of light in vacuum and $\mathbf{r} = x\hat{\imath} + y\hat{\jmath}$ is independent of z.

The periodicity in the x-direction is another symmetry condition that is considered. Due to this property and the form of the differential equation Eq. (1) the Bloch theorem can be applied for the x-direction. In this way the following expression can be derived

$$\Psi(x - P, y) = \exp(-ikP)\, \Psi(x, y), \tag{2}$$

where k is the one-dimensional Bloch vector.

To determine the band structure we have to find the dispersion relation $\omega = \omega(k)$. With this in mind, let us consider a Green's function for a bidimensional geometry that can be used to solve the Helmholtz equation. The Green's function considered is $G(\mathbf{r},\mathbf{r}') = i\pi H_0^{(1)}(k|\mathbf{r}-\mathbf{r}'|)$, where $H_0^{(1)}(\varrho)$ is the Hankel function of the first kind and zero order. Considering the geometry of the unit cell shown in Fig. 1 and applying the two-dimensional second Green's theorem for the functions Ψ and G we obtain the expression

$$\frac{1}{4\pi}\oint_{\Gamma}\left[G(\mathbf{r},\mathbf{r}')\frac{\partial\Psi(\mathbf{r}')}{\partial\mathbf{n}'}-\frac{\partial G(\mathbf{r},\mathbf{r}')}{\partial\mathbf{n}'}\Psi(\mathbf{r}')\right]ds'=\theta(\mathbf{r})\,\Psi(\mathbf{r}), \quad (3)$$

being $\theta(\mathbf{r})=1$ if $\mathbf{r}$ is inside the unit cell and $\theta(\mathbf{r})=0$ otherwise. ds' is the differential arc's length, $\mathbf{n}'$ is the outward normal vector to Γ, and the observation point $\mathbf{r}$ is infinitesimally separated of contour Γ outer to the unit cell. The geometry of the problem is described by representing the points along the contour Γ with Cartesian coordinates $X(s')$, $Y(s')$ as parametric functions of the arc's length s' and their derivatives $X'(s')$, $Y'(s')$, $X''(s')$ and $Y''(s')$, up to second order.

To solve numerically Eq. (3), we divide the curve Γ in four segments Γ_1, Γ_2, Γ_3 and Γ_4 (Fig. 1) and take a sampling $X_n = X(s_n)$, $Y_n = Y(s_n)$ along the each curve. The corresponding number of points along the curves are N_1, N_2, N_3 and N_4 respectively and we call $N = N_1+N_2+N_3+N_4$ to the total number of points. It is worth mentioning that the points (X_n, Y_n) on Γ_3 must be corresponding to those on Γ_4 $(X_n - P, Y_n)$, in this way $N_3 = N_4$. Besides these considerations, we take into account the boundary condition at the PEC surfaces (with curves Γ_1 and Γ_2). In this way, Eq. (3) can be represented numerically in terms of a homogeneous system of N algebraic equations as follows:

$$\sum_{n=1}^{N_1}L_{mn(1)}\Phi_{n(1)}+\sum_{n=1}^{N_2}L_{mn(2)}\Phi_{n(2)}+\sum_{n=1}^{N_3}L_{mn(3)}\Phi_{n(3)} - \sum_{n=1}^{N_3}N_{mn(3)}\Psi_{n(3)}+\sum_{n=1}^{N_4}L_{mn(4)}\Phi_{n(4)}-\sum_{n=1}^{N_4}N_{mn(4)}\Psi_{n(4)}=0, \quad (4)$$

for $m = 1, 2, \ldots, N$. In the Eq. (4) the source functions $\Psi_{n(3)}$ and $\Phi_{n(j)}$ represent numerically the field Ψ and its normal derivative, besides, the subscripts $n(j)$, $j = 1, 2, 3, 4$ denote the n-th point along the Γ_j contour. The matrix element $L_{mn(j)}$ and $N_{mn(j)}$ are given by [19, 21]

$$L_{mn(j)} = i\frac{\Delta s}{4}H_0^{(1)}\left(\frac{\omega}{c}d_{mn}\right)(1-\delta_{mn})+i\frac{\Delta s}{4}H_0^{(1)}\left(\frac{\omega}{c}\frac{\Delta s}{2e}\right)\delta_{mn}, \quad (5)$$

and

$$N_{mn(j)} = i\frac{\Delta s}{4}\frac{\omega}{c}H_1^{(1)}\left(\frac{\omega}{c}d_{mn}\right)\frac{D_{mn}}{d_{mn}}\left(1-\delta_{mn}\right)+\left(\frac{1}{2}+\frac{\Delta s}{4\pi}D'_n\right)\delta_{mn}, \tag{6}$$

where

$$d_{mn} = \sqrt{\left(X_m - X_n\right)^2 + \left(Y_m - Y_n\right)^2}, \tag{7}$$

$$D_{mn} = -Y'_n\left(X_m - X_n\right) + X'_n\left(Y_m - Y_n\right), \tag{8}$$

$$D'_n = X'_n Y''_n - X''_n Y'_n. \tag{9}$$

$H_1^{(1)}(\varrho)$ is the Hankel's function of first kind and first order. The function $\delta_{mn}^{(j)}$ represents the Kronecker's delta and Δs is the arc's length between two consecutive points of a given curve. In Eqs. (8) and (9), we have defined $X'_n = X'(s)|_{s=s_n}$, $X''_n = X''(s)|_{s=s_n}$, and so forth. For simplicity we have omitted the contour index (j) but it must be implicitly understood that $n = n(j)$ wherever it appears in Eqs. (5)–(9).

By applying Eq. (2), we obtain the equations $\Psi_n^{(4)} = \exp(-ikP)\,\Psi_n^{(3)}$, and $\Phi_n^{(4)} = -\exp(-ikP)\,\Phi_n^{(3)}$. The minus sign appearing in last equation results because the normals to corresponding points at Γ_3 and Γ_4 have opposite directions. With these equations we have

$$\sum_{n=1}^{N_1} L_{mn(1)}\Phi_{n(1)} + \sum_{n=1}^{N_2} L_{mn(2)}\Phi_{n(2)} + \sum_{n=1}^{N_3}\left(L_{mn(3)} - \exp(-ikP)\,L_{mn(4)}\right)$$

$$\times\Phi_{n(3)} - \sum_{n=1}^{N_3}\left(N_{mn(3)} + \exp(-ikP)\,N_{mn(4)}\right)\Psi_{n(3)} = 0, \tag{10}$$

with $m = 1, 2, \ldots, N$. Eq. (10) constitutes a linear system that has an associated representative matrix, M_{mn}, that depends on the frequency ω and the Bloch vector k. Since the equation system is homogeneous, a nontrivial solution can be obtained if the determinant of such matrix is zero. If we define the function

$$D(k,\omega) = \ln\left(\left|\det(M)\right|\right). \tag{11}$$

Numerically this function presents local minimum points that will give us the numeric dispersion relation $\omega = \omega(k)$ that determines the band structure.

In the dispersion relation of the system that we are considering, the one-dimensional Bloch vector is present in view of the periodicity in a certain direction. We wonder at this point how we could recognize when a physical system is a photonic crystal?

To answer this question, let us consider the following: the photonic crystal's response is determined by the existence of a dispersion relation that is a function of a Bloch vector, regardless of the specific configuration of our physical system. In this sense our waveguide with periodic roughness acts as a photonic crystal.

In addition to the above, we can observe that the electromagnetic radiation is transmitted through the waveguide in a bounded region and then, our system has a dual role: one as a photonic crystal and the other as a waveguide.

A wide variety of waveguides and optical fibers that also function as photonic crystals are presented in the book of Joannopoulos [24]. In all these cases the photonic crystals are made by introducing periodic variation of the dielectric function.

In contrast, in the system we are proposing, the response of a 1D photonic crystal is achieved without considering of such variation. Instead we introduce a structure on the surfaces of a hollow metallic waveguide that indeed has the optical response of a photonic crystal.

We started from the idea of an infinite length system, which has a dispersion relation similar to that of some well known photonic crystals. The waveguide of finite length can be considered as a truncated photonic crystal, when the number of periods is properly chosen.

The idea of using rough surfaces to fabricate photonic crystals is particularly relevant when one considers the existence of a well-developed technology for manufacturing surfaces with a given profile, see reference [25].

In order to calculate the field distribution within a unit cell for a resonant mode at a given point (k, ω), we consider the following two step procedure: In the first step we find numerically the source functions by solving the homogeneous equations system by using the SVD (singular value decomposition). In the second step we substitute these functions (numerical version of Eq. (3)) to obtain the field $\Psi(\mathbf{r})$ at any point within the unit cell.

To model the system we assume an infinite periodic waveguide in the x-direction. The band structure associated to this waveguide resembles those obtained for a one-dimensional photonic crystal [23]. In this work, we are particularly interested in the band gaps. In practice a waveguide will have a finite length, so we will verify the existence of band gaps by modeling the reflectivity with the integral method in very much the same as we do with truncated photonic crystals [19, 21].

Let us consider the problem of calculating the reflectance of a finite length waveguide that is illuminated with an incident field $E_{inc}(\mathbf{r}, t) = \Psi_{inc}(\mathbf{r}) e^{-i\omega t}$ as sketched in Fig. 3. In this case the Green's

integral theorem for the region R_0 takes the form

$$\Psi(\mathbf{r}) = \Psi_{inc}(\mathbf{r}) + \frac{1}{4\pi}\int\limits_{\Gamma_1} G\left(\mathbf{r},\mathbf{r}'\right)\frac{\partial\Psi(\mathbf{r}')}{\partial\mathbf{n}'}ds' - \frac{1}{4\pi}\int\limits_{\Gamma_2}\frac{\partial G(\mathbf{r},\mathbf{r}')}{\partial\mathbf{n}'}\Psi(\mathbf{r}')ds', \tag{12}$$

where Γ_1 and Γ_2 are curves corresponding to the perfect conductor surfaces and $\mathbf{n}'$ is the outward normal vector.

To determine numerically the field and its normal derivative involved in last equation we solve the non homogeneous system of algebraic equations. Details of the numerical method can be found in Refs. [20, 26–28].

To treat the problem with the numerical method given above, some considerations must be made. Since the size of the system is finite, to avoid edge effects we illuminate it with a tapered Gaussian beam whose intercept with the plane of the channel has a half-width g. This parameter must be smaller than the total length of the system $L_y = 2l + b$, but much larger than the width of the aperture b (see Fig. 3).

With these considerations, the incident field can be expressed in terms of its angular spectrum $A(q, k_\parallel)$

$$\Psi_{inc}(x,y) = \int\limits_{-\omega/c}^{\omega/c}\frac{dq}{2\pi}A(q,k_\parallel)\exp\{i\left[qx - \alpha_0(q)y\right]\}, \tag{13}$$

where $\alpha_0(q) = [(\omega/c)^2 - q^2]^{1/2}$ with $\Re e\,\alpha_0(q) > 0$ and $\Im m\,\alpha_0(q) > 0$. In this work, we choose

$$A(q,k_\parallel) = \sqrt{\pi}g\exp\left\{-g^2(q-k_\parallel)^2/4\right\}, \tag{14}$$

where the parameter $k_\parallel = (\omega/c)\sin\theta_0$, being θ_0 the angle of incidence (see Fig. 3).

With this incident field we can find that the total power crossing the area L_xL_z is:

$$P_{inc}(k_\parallel) = L_z\sqrt{\frac{\pi}{2}}\,g\,\alpha_0(k_\parallel)\frac{c^2}{8\pi\omega},$$

where we have assumed that $(\omega/c)g \gg 1$.

Therefore, using the plane-wave expansion [26] to calculate the z-component of the Poynting vector, we find the following expression for the total scattered power

$$P_{sc}\left(k_\parallel\right) = L_z\frac{c^2}{8\pi\omega}\int\limits_{-\omega/c}^{\omega/c}\frac{dq}{2\pi}\alpha_0(q)|S(q,k_\parallel)|^2\,.$$

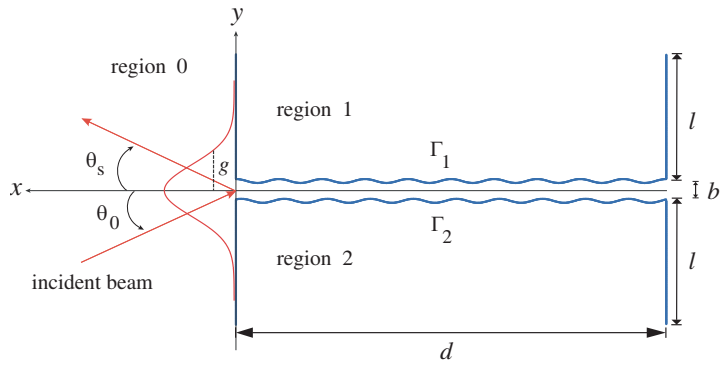

Figure 3. Schematic description of the tunnel of width b and length d with corrugated surfaces is illuminated by a Gaussian beam in region 0. Regions 1 and 2 constitute the perfect conductor. The $1/e$ half-width of the modulus of the incident Gaussian beam projected on the plane $x = 0$ is g. The angles of incidence θ_0 and scattering θ_s for reflection are also shown.

Then, reflectance is given by

$$R\left(k_{\parallel}\right) = \frac{P_{sc}(k_{\parallel})}{P_{inc}(k_{\parallel})} = \frac{1}{\mathcal{F}(k_{\parallel})} \int_{-\omega/c}^{\omega/c} \frac{dq}{2\pi} \alpha_0(q) \left|S(q, k_{\parallel})\right|^2 , \tag{15}$$

where

$$\mathcal{F}\left(k_{\parallel}\right) = \sqrt{\frac{\pi}{2}}\, g\, \alpha_0\left(k_{\parallel}\right) , \tag{16}$$

and

$$S\left(q|k_{\parallel}\right) = -\frac{i}{2\alpha_0(q)} \sum_{j=1}^{2} \left[\int_{\Gamma_j} F \exp\left\{-i\left[qx + \alpha_0(q) y\right]\right\} ds \right] . \tag{17}$$

For propagating waves, we can identify the components of the wave vector as $q = \omega/c \sin\theta_s$ and $\alpha_0(q) = \omega/c \cos\theta_s$, where θ_s is the scattering angle (see Fig. 3).

3. RESULTS

In this section, we present a numerical study of the proposed system.

To start this study we consider a waveguide with flat walls. This system indeed has band structure that can be calculated analytically.

To validate the numerical method presented in the previous section, we compare the analytical results with those obtained numerically.

The waveguide (with flat walls) has a width b and infinite length. This system has an arbitrary period. The dispersion relation in this case is given by [17]

$$\omega(k) = c\sqrt{\left(k+\frac{2\pi n}{P}\right)^2+\left(\frac{m\pi}{b}\right)^2}, \quad n=\pm1,\pm2,\ldots \text{ and } m=1,2,\ldots \tag{18}$$

The dispersion relation given by this equation is similar to that of a photonic crystal slab, where the finite thickness in the y-direction gives rise to a different behavior of that presented by the infinite system. When we compare this system with the case of one-dimensional photonic crystals. Let us consider the following analysis by using this equation. The right hand side of Eq. (18) has two terms inside the square root symbol. The first one represents the band structure in the first Brillouin zone. This term depends on a single component of the Bloch vector and an integer. The second term is present because the system is finite in the y-direction, and depends on the integer m. In this case, the frequency depends on a continuous variable and two discrete variables.

A one-dimensional photonic crystal has a dispersion relation that depends only on a continuous variable (Bloch vector) and a discrete variable, this is because there is no restriction in the y-direction. Therefore the band structures that we show in this work are more complex than the structures that typically arise in the one-dimensional case, and some of our results resemble the band structures of two-dimensional photonic crystals. However, in the case of two-dimensional photonic crystals the frequency depends on two continuous variables (the two components of the Bloch vector) and two discrete variables. This leads to different physical phenomena that can not be present in our system since we have a Bloch vector with one component instead of two.

In Fig. 4, we show the band structure in terms of the reduced frequency $\omega_n = (P/2\pi)(\omega/c)$ and k within the first Brillouin zone $-\pi/P \leq k \leq \pi/P$, with $P = 2\pi$, determined with our numerical method. In this case $b = 3$ (arbitrary units). The band structure analytically determined by using Eq. (18) is overlapped to the first one showing an excellent agreement.

The reason for the modes to appear overlapped giving a more complex band structure (compared to those associated with a 1DPC) results from the constraint of the system in the y-direction which is related to the integer m that appears in Eq. (18). This features

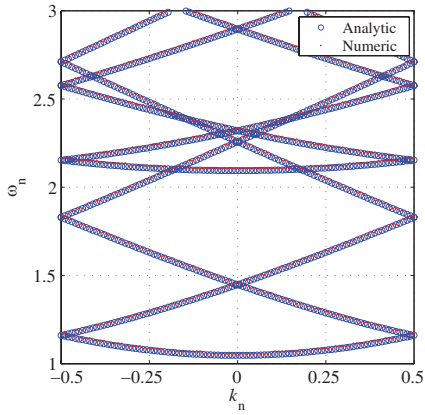

Figure 4. Band structure of a tunnel with flat walls. Comparison of analytical (circles) and numerical modeling (dots).

resemble those appearing in the band structure associated to two-dimensional photonic crystals where the dispersion relation depends on a Bloch wave vector with two components.

The variation of amplitude and phase difference of the roughness leads notable changes in the band structure as will be shown below. In Fig. 5(a), we present the band structure of a waveguide with the parameters $b = 3$, $P = 2\pi$, $A_1 = A_2 = A = 0.1b$ and $\Delta\phi = 0$ under TE polarization. Since the frequency range for large wavelengths and relatively small amplitudes of roughness are being considered, we observe few changes in the band structure compared to that produced by waveguides with flat walls (Fig. 4). Narrow complete gaps appear in the structure, even though it is not clear in the figure.

We can obtain important changes in the band structure by introducing a simple change of phase difference $\Delta\phi = \pi/2$ as shown in Fig. 5(b). Particularly, in this figure is very important to observe the widening of gaps. Moreover, it is important to notice that the band structures shown have a certain similarity to those associated with two-dimensional photonic crystals rather than those present in one-dimensional systems. Despite the system under study needs only one component of the Bloch wave vector to be described, the given boundary conditions along the y-axis work out more complex band structures than that obtained in the study of 1DPC which are not restricted in such direction.

The influence of the amplitude of the surface roughness in the band structure is shown in Figs. 6(a) and 6(b). In this case, the amplitude was $A = 0.2b$ and we considered two phase differences $\Delta\phi = 0$ and $\Delta\phi = \pi/2$, respectively. It is worth noticing that in

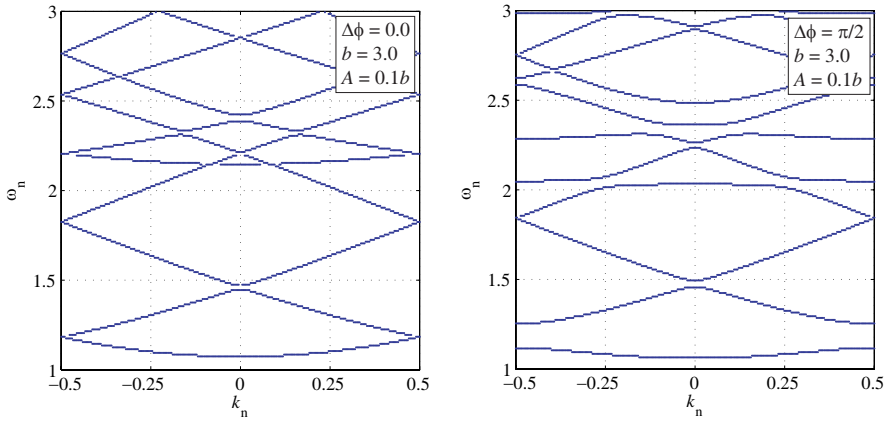

Figure 5. Band structure of the tunnel with a width $b = 3$ and periodic amplitudes $A = 0.1b$ with a phase difference (a) $\Delta\phi = 0$ and (b) $\Delta\phi = \frac{\pi}{2}$ under TE polarized illumination.

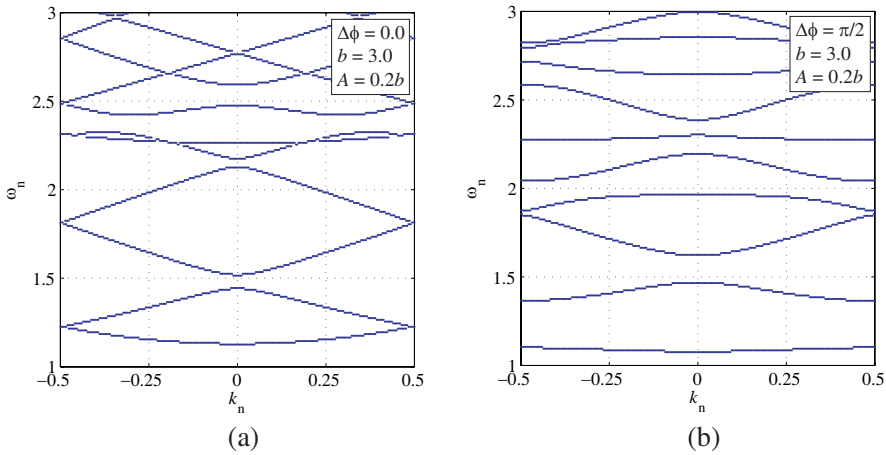

Figure 6. Band structure of the tunnel with a width $b = 3$ and periodic amplitudes $A = 0.2b$ with a phase difference (a) $\Delta\phi = 0$ and (b) $\Delta\phi = \frac{\pi}{2}$ under TE polarized illumination.

this case it is also possible to widen the gaps. It is obvious that the major changes on the band structure are due to appreciable changes in the roughness amplitudes and phase differences, as can be seen in Fig. 6(b). Despite the effects of varying the phase difference or the amplitudes are almost the same, we will discuss below why could be

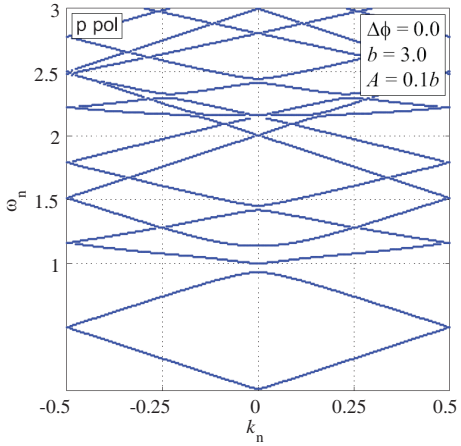

Figure 7. Band structure of the tunnel with a width $b = 3$ and periodic amplitudes $A = 0.1b$ with a phase difference $\Delta\phi = 0$ under TM polarized illumination.

more practical to manipulate the phase difference.

Under TM polarization the simulation shows analogous results. Varying the parameters of the waveguide results in a widening (or narrowing) of gaps. In Fig. 7, we show an example of a band structure under TM polarization. The parameters considered were those of the example given in Fig. 5(a).

In previous results, we assumed an infinite length waveguide. However, the waveguides we can analyze experimentally are of finite length. So, we would like to see if the gaps in the band structure of the ideal waveguide (infinite in length) appear in the case of a waveguide of finite length. Let us consider a finite length waveguide (see Fig. 3) with $d = 20\pi$ (only 10 periods), $l = 10\pi$ with the parameters: $b = 3$, $P = 2\pi$, $A = 0.2b$, $\Delta\phi = \pi/2$. In Fig. 8, we show the reflectance of the system under TE polarization when a Gaussian beam of a half-width $g = 11.2$ illuminates the waveguide under normal and oblique incidence $\theta_0 = 0°$ (solid line) $\theta_0 = 20°$ (dashed line) respectively. It is worth observing that in both cases the reflectance is quite high in the regions quoted by the extrema of the dispersion curves (Fig. 6(b)), so, these are complete gaps. Some few periods are needed to get a high reflectance response corresponding to the frequency regions of gaps. It is important to observe that the numerical methods used to determine the band structure and the reflectance are independent, although they have in common the use of the Green's theorem. This means that both methods validate between them, at least for the presented simulations.

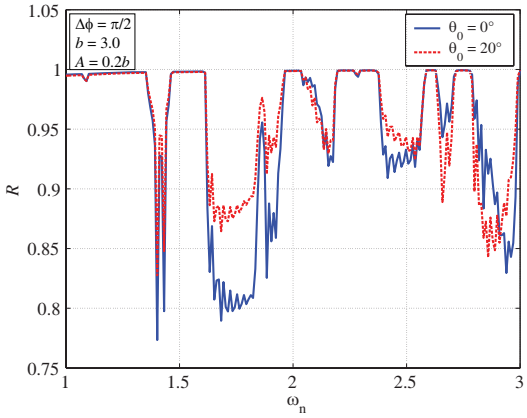

Figure 8. Reflectance of the tunnel illuminated with a Gaussian beam. The thickness of the tunnel is $b = 3$ with a phase difference $\Delta\phi = \frac{\pi}{2}$ in corrugated surfaces and the $1/e$ half-width of the projection of the beam on the left side of the tunnel is $g = 11.2$. The solid curve corresponds to normal incidence $\theta_0 = 0°$, the dashed curve to oblique incidence $\theta_0 = 20°$.

3.1. Discrete Modes

Numerical simulations show that for a given phase difference in general an increase on the roughness amplitude widens the gaps. This fact implies that the mode curves become flatter, so, the modes can be associated to discrete frequencies since only discrete modes are allowed inside the waveguides. This effect will start from low frequencies, so, we refer to discrete modes for a given interval of frequencies. This is shown in Fig. 9 which was obtained using the parameters of the example given in Fig. 6(b) with $A = 0.3b$. The presence of discrete states (Fig. 9) is confirmed by the reflectance results as shown in Fig. 10, where we observe a narrow drop on the reflectance around the frequency corresponding to the second mode.

One of the most important factors for the presence of discrete states in our system is that the surfaces are assumed to be perfect conductors. Although in the case of real conductors such states do not appear. However, for a conductor with a high conductivity we can choose the system parameters so that some allowed bands are very narrow.

The intensity of the electric field within a unit cell is shown in Figs. 11(a) and 11(b), for a system with the same parameters of previous system for the frequencies $\omega_n = 1.100$ and $\omega_n = 1.467$,

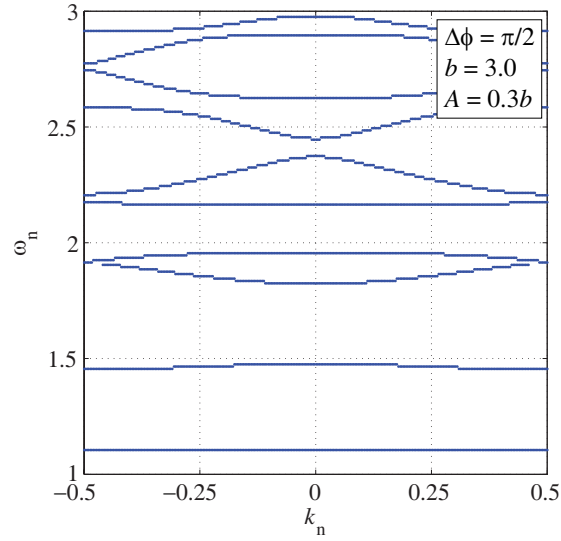

Figure 9. Band structure of the tunnel with a width $b = 3$ and periodic amplitudes $A = 0.3b$ with a phase difference $\Delta\phi = \frac{\pi}{2}$ under TE polarized illumination.

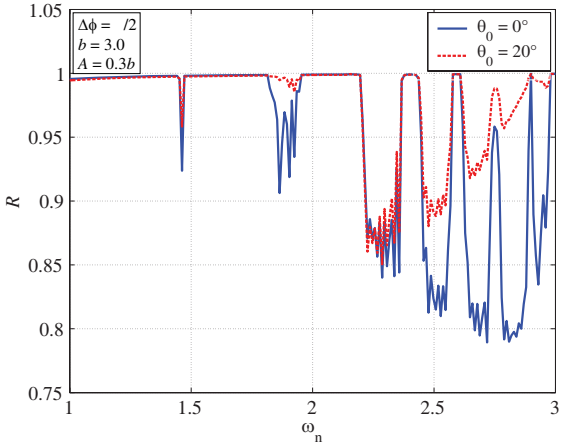

Figure 10. Reflectance of the tunnel illuminated with a Gaussian beam. The thickness of the tunnel is $b = 3$ with a phase difference $\Delta\phi = \frac{\pi}{2}$ in corrugated surfaces and amplitudes $A = 0.3$. The solid curve correspond to normal incidence $\theta_0 = 0°$, the dashed curve to oblique incidence $\theta_0 = 20°$.

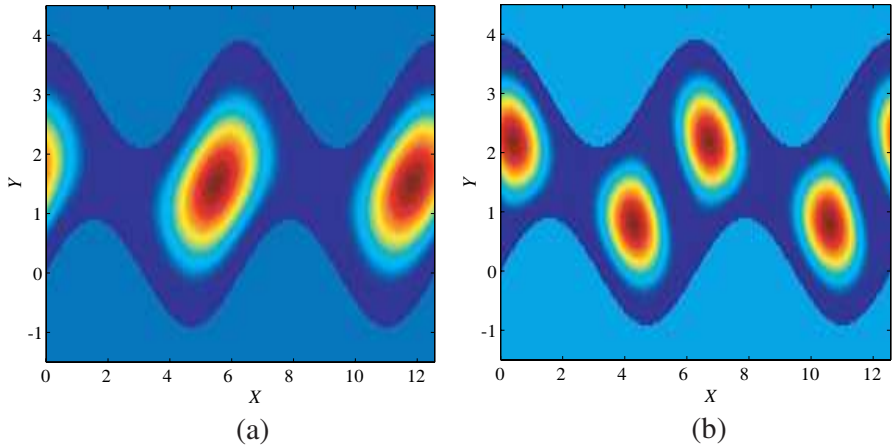

Figure 11. Scattered field belongs to a cell with the same parameters of previous system for the frequencies (a) $\omega_n = 1.100$ and (b) $\omega_n = 1.467$.

respectively. The Fig. 11(a) corresponds to the first discrete state that appears in the band structure of Fig. 9. To observe this state, it would be necessary to increase the resolution of this graph.

To corroborate the presence of discrete modes that can propagate through the finite waveguide, we calculated the intensity of the electric field within the waveguide under normal incidence (see Fig. 12). In Fig. 12, we show the scattered field associated to a waveguide of length $d = 20\pi$, for the frequency $\omega_n = 1.467$.

Figure 13 was obtained by considering the parameters $\Delta\phi = \pi$, $b = 3$, and $A = 0.4b$. In this case, the discrete modes become more evident. In this figure, the bands seem to be horizontal lines (discrete modes), however, if we use a higher resolution such bands should have some curvature. Actually the meaning of discrete states since a numerical point of view is relative to a given resolution.

The existence of these states can be understood by taking into account various arguments. For relatively high amplitudes the waveguide is almost closed, so, the transmission of the electromagnetic wave through the waveguide is very weak. In fact, the transmittance for all these states is quite low. By considering that the mode is an electromagnetic field that must satisfy some given boundary conditions, those that correspond to long wavelengths (low frequencies) find more difficulty in coupling to the waveguide. This is the reason why discrete states appear mostly in the lower part of the band structure. Recalling that in solid state physics it is possible to represent

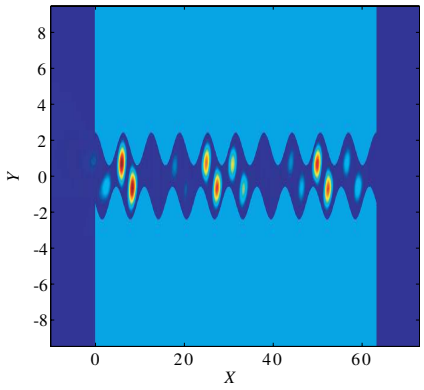

Figure 12. Scattered field belongs to a perfectly conductor tunnel of length $d = 20\pi$, for the frequency $\omega_n = 1.467$.

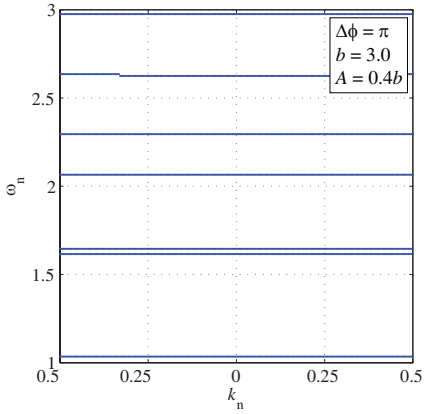

Figure 13. Band structure of the tunnel with a width $b = 3$ and periodic amplitudes $A = 0.4b$ with a phase difference $\Delta\phi = \pi$ under TE polarized illumination.

a band structure as a function of the lattice parameter. When this parameter is large, the atoms are far away from each other, so, the interaction is weak. The energy bands become very thin resulting in discrete states of isolated atoms. We believe that in the case of waveguides, when the unit cells gradually tend to close, the existence of modes is dependent on each isolated cell appearing then these discrete modes.

Our interest in this work, is to propose a system based on this waveguide with a periodic roughness on its surfaces in such a way that the band structure and the reflectance can be manipulated in an interesting way for practical purposes. This system can be set up to work in the optical spectrum with existing technology. If the device is on the microscopic scale, it would be desirable to show the presence of band gaps even in the case that we have a finite corrugated section of the waveguide, despite the smooth walls of the waveguide extend over a large length in the scale of millimeters. In Fig. 14, we show the reflectance obtained for a long waveguide, as sketched in the inset of Fig. 14. The total length of the smooth part of the waveguide is $s = 20\pi$ with the parameters used to model the system shown in Fig. 10.

It is important to notice the good agreement of the high reflectance regions within the gap regions. This result makes evident that it is possible to carry out this system to practical purposes.

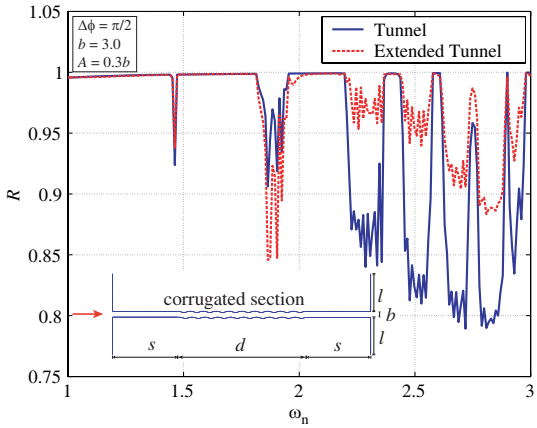

Figure 14. Reflectance of a tunnel with flat walls of length $s = 20\pi$ (solid line) and only a short section with corrugated surfaces of length $d = 20\pi$ (dashed line). Results compared with the reflectance of the system given in Fig. 10 under normal incidence.

We mentioned that it is more practical to manipulate the phase difference rather than the amplitude of the roughness. This comment would apply to a manufactured device consisting of two periodic surfaces. Obviously is impractical to be changing the morphology of surfaces, if we want to obtain modifications to the band structure. In contrast, to change the phase difference the device could have a mechanism to allow the relative translation between the surfaces in the direction of the periodicity. This mechanism could be like to the micrometer drive in a Michelson interferometer.

4. CONCLUSION

We have applied an integral numerical method to analyze the optical response of a corrugated periodic waveguide with perfect electric conductor walls. With this method we determined the band structure and the reflectance of this system.

The band structure of this waveguide resembles that associated to one-dimensional photonic crystals, with some interesting features that allow to manipulate the band structure, particularly the gaps width by just changing the phase difference or the amplitude of the surface profiles. This properties present some interest since a technological point of view.

We have found also that as the waveguide becomes narrow and

narrow the modes get the properties of discrete modes in very much the same as happens with atoms in isolated state.

Despite the band structure of the proposed system is similar in some features to those associated to a one-dimensional photonic crystal, it presents a more complex and interesting band structure that results from the constraint of the system in the y-direction.

ACKNOWLEDGMENT

Alberto Mendoza-Suárez expresses his gratitude to the Coordinación de la Investigación Científica de la Universidad Michoacana de San Nicolás de Hidalgo, for the support to this research.

REFERENCES

1. Elliot, R. S., "On the theory of corrugated plane surfaces," *IRE Trans. AP*, Vol. 2, 71–81, 1954.
2. Jancewicz, B., "Plane electromagnetic wave in PEMC," *Journal of Electromagnetic Waves and Applications*, Vol. 20, No. 5, 647–659, 2006.
3. Lindell, I. V. and A. H. Sihvola, "The PEMC resonator," *Journal of Electromagnetic Waves and Applications*, Vol. 20, No. 7, 849–859, 2006.
4. Lindell, I. V. and A. H. Sihvola, "Reflection and transmission of waves at the interface of perfect electromagnetic conductor (PEMC)," *Progress In Electromagnetics Research B*, Vol. 5, 169–183, 2008.
5. Imran, A., Q. A. Naqvi, and K. Hongo, "Diffraction of electromagnetic plane wave from a slit in PEMC plane," *Progress In Electromagnetic Research M*, Vol. 8, 67–77, 2009.
6. Zhang, G., H. Zhang, Z. Yuan, Z. Wang, and D. Wang, "A novel broadband E-plane omni-directional planar antenna," *Journal of Electromagnetic Waves and Applications*, Vol. 24, No. 5–6, 663–670, 2010.
7. Liu, Y. and S.-X. Gong, "Design of a compact broadband double-ridged horn antenna," *Journal of Electromagnetic Waves and Applications*, Vol. 24, No. 5–6, 765–774, 2010.
8. Hammou, D., E. Moldovan, and S. O. Tatu, "V-band microstrip to standard rectangular waveguide transition using a substrate integrated waveguide (SIW)," *Journal of Electromagnetic Waves and Applications*, Vol. 23, No. 2–3, 221–230, 2009.

9. Shelby, R. A., D. R. Smith, and S. Schultz, "Experimental verification of a negative index of refraction," *Science*, Vol. 292, 77–79, 2001.
10. Pendry, J. B., L. Martín-Moreno, and F. J. García-Vidal, "Mimicking surface plasmons with structured surfaces," *Science*, Vol. 305, No. 5685, 847–848, 2004.
11. García-Vidal, F. J., L. Martín-Moreno, and J. B. Pendry, "Surfaces with holes in them: New plasmonic metamaterials," *J. Opt. A: Pure and Appl. Opt.*, Vol. 7, S97–S101, 2005.
12. García de Abajo, F. J. and J. J. Sáenz, "Electromagnetic surface states in structured perfect-conductor surfaces," *Phys. Rev. Lett.*, Vol. 95, 233901, 2005.
13. Qiu, M., "Photonic band structures for surface waves on structured metal surfaces," *Opt. Express*, Vol. 13, No. 19, 7583–7588, 2005.
14. Oh, S. S., S.-G. Lee, J.-E. Kim, and H. Y. Park, "Self-collimation phenomena of surface waves in structured perfect electric conductors and metal surfaces," *Opt. Express*, Vol. 15, No. 3, 1205–1210, 2007.
15. Inoue, K. and K. Ohkata, *Photonic Crystals*, Springer, Germany, 2004.
16. Maradudin, A. A. and A. R. McGurn, "Photonic band structure of a truncated, two-dimensional, periodic dielectric medium," *J. Opt. Soc. Am. B*, Vol. 10, No. 2, 307–313, 1993.
17. Luna-Acosta, G. A., K. Na, L. E. Reichl, and A. Krokhin, "Band structure and quantum Poincaré sections of a classically chaotic quantum rippled channel," *Phys. Rev. E*, Vol. 53, No. 4, 3271–3283, 1996.
18. Herrera-González, I., G. Arroyo-Correa, A. Mendoza-Suárez, and E. Tútuti-Hernández, "Study of the resistivity in a channel with dephased ripples," *Int. J. Mod. Phys. B*, Vol. 25, No. 5, 683–698, 2011.
19. Mendoza-Suárez, A., F. Villa-Villa, and J. A. Gaspar-Armenta, "Numerical method based on the solution of integral equations for the calculation of the band structure and reflectance of one- and two-dimensional photonic crystals," *J. Opt. Soc. Am. B*, Vol. 23, No. 10, 2249–2256, 2006.
20. Pérez, H. I., E. R. Méndez, C. I. Valencia, and J. A. Sánchez-Gil, "On the transmission of diffuse light through thick slits," *J. Opt. Soc. Am. A*, Vol. 26, No. 4, 909–918, 2009.

21. Mendoza-Suárez, A., F. Villa-Villa, and J. A. Gaspar-Armenta, "Band structure of two-dimensional photonic crystals that include dispersive left-handed materials and dielectrics in the unit cell," *J. Opt. Soc. Am. B*, Vol. 24, No. 12, 3091–3098, 2007.
22. Villa-Villa, F., J. A. Gaspar-Armenta, and A. Mendoza-Suárez, "Surface modes in one dimensional photonic crystals that include left handed materials," *Journal of Electromagnetic Waves and Applications*, Vol. 21, No. 4, 485–499, 2007.
23. Villa-Villa, F., J. A. Gaspar-Armenta, and F. Ramos-Mendieta, "One-dimensional photonic crystals — Equivalent systems to single layers with a classical oscillator like dielectric function," *Optics Comm.*, Vol. 216, 361–367, 2003.
24. Joannopoulos, J. D., S. G. Johnson, J. N. Winn, and R. D. Meade, *Photonic Crystals: Molding the Flow of Light*, Princeton University Press, New Jersey, 2008.
25. Méndez, E. R., M. A. Ponce, V. Ruiz-Cortés, and Z. H. Gu, "Photofabrication of one-dimensional rough surfaces for light scattering experiments," *Appl. Opt.*, Vol. 30, No. 28, 4103–4113, 1991.
26. Maradudin, A. A., T. Michel, A. R. McGurn, and E. R. Méndez, "Enhanced backscattering of light from a random grating," *Ann. Phys.*, Vol. 203, No. 2, 255–307, 1990.
27. Mendoza-Suárez, A. and E. R. Méndez, "Light scattering by a reentrant fractal surface," *Appl. Opt.*, Vol. 36, No. 15, 3521–3531, 1997.
28. Valencia, C. I., E. R. Méndez, and B. S. Mendoza, "Second-harmonic generation in the scattering of light by two-dimensional particles," *J. Opt. Soc. Am. B*, Vol. 20, No. 10, 2150–2161, 2003.